

**MINERALOGY AND PETROLOGY REPORT**

No. 85/12

Vanadiferous nodules from the Littleham Marl  
near Budleigh Salterton, Devon.

by P.H.A. Muncarrow

with appendix on XRF analyses by D.J. Bland.

**Mineral Sciences and Isotope Geology Research Group**

**British Geological Survey**

**64-78 Gray's Inn Road**

**London WC1X 8NG**

This report has been generated from a scanned image of the document with any blank pages removed at the scanning stage.  
Please be aware that the pagination and scales of diagrams or maps in the resulting report may not appear as in the original

Vanadiferous nodules from the Littleham Marl near Budleigh Salterton, Devon.

### Introduction

A collection of nodules from the Littleham Marl sequence near Budleigh Salterton was submitted for investigation of their composition and mineralogy (13 specimens, table A). Initially, three were selected for sectioning and analysis, but preliminary results revealed such wide variations in composition and mineralogy that a qualitative study of the collection was followed by fuller analyses of some examples which showed significant concentrations of elements of interest such as U, V, Cu, Co and Ag. Techniques used included XRF, electron microprobe, XRD, and evolved gas analysis. In this instance, microprobe analysis was confined to point analyses of selected mineral grains due to the restricted time available. Detailed multi-element line scans or area imaging using the microprobe would have been inordinately time consuming for the comparatively large surface areas of these specimens. Further work on this aspect might be carried out using SEM techniques.

### General description

The nodules occur in a moderate reddish brown sandy marl with some thin lenticles of more sandy sediment with only a little clay matrix, and small irregular patches or fine laminae of silty or clayey material. They are varied in character, from small dark spots at the centres of grey reduction spheres in the red marl, to dense dark brown to black concretions surrounded by grey haloes. Grey reduction spots with no dark cores are also common. The colour change at the boundary is sharp, in some cases down to a scale of a few  $\mu\text{m}$ , and passes across sedimentary features such as silty laminae with very little if any, deviation. The dark concretions are near spherical to ellipsoidal in shape, and commonly

Table A. list of nodules

PTS

HER 8000a	Nodule (5 cm) from wave-cut platform. Littleham Cove. _____	9106
8000b	Nodule (6 cm) Littleham Cove. Almost perfect sphere. _____	9232
8000c	Slightly flattened nodule (4 cm). Littleham Cove. _____	-
8000d	Nodule (3 cm). Littleham Cove. _____	-
8000e	Flattened Nodule (6 cm). Littleham Cove. _____	9107
8000f	Flattened Nodule (5 cm). Littleham Cove. _____	9235
HER 8009	Nodule (?), Liverton Branch of Stream, Withycombe Rayleigh	-
HER 8010	Pea-sized nodules from housing estate, Withycombe Rayleigh	9237
HER 8014	Flattened nodule in surrounding mudstone, Combe Farm stream.	9238
HER 8023	'Fish-eye', Littleham Cove. _____	-
HER 8026	Small nodule in fine sst/mudstone, Sandy Bay _____	9239
HER 8045	Nodule (5 cm), Aylesbeare (SY 0335 9152). _____	9240
HER 8046	Nodule (3 cm), Aylesbeare (SY 0331 9154). _____	9108

HER ..... collector's numbers

PTS polished thin section numbers

of the order of 2 to 6 cm diameter. Some of these have a distinct concentric zoned structure with alternating dark and light bands conspicuous on a cut surface but less obvious in this section. Others have irregular bands and patches of dark colour, and some are evenly dark throughout. These colour variations are due to concentrations of opaque or dark minerals, and to colour differences in the clay matrix.

The concretions with an ellipsoidal form are flattened approximately parallel to the rather indistinct bedding, and some have thin equatorial fins of dark material extending into the bleached halo zone of the nodule. It has been suggested (Harrison, R.K., 1975) that these finned edges represent distortion of the concretion during postdepositional compaction of the sediment and that the more spherical nodules are of later (ie post-compaction) formation. During the course of the present study, no significant chemical or mineralogical features were found which conclusively support or refute the view of a later origin for the spherical nodules. In the suite from Littleham Cove, for example, two spherical nodules of similar size, HBR 8000a and 8000b show widely differing features (see tables 2, 22, and sample notes) whereas 8000f, a flattened nodule, shows close similarities to 8000a. A significant factor may be the degree of weathering, 8000a and f being dark, hard, and rich in fine opaques, including sulphides, and apparently only slightly weathered, while 8000b is softer, more friable, paler and more brown in colour, and has few opaques outside the 2mm core. It is noteworthy however, that despite the flattened and "finned" appearance of 8000f in hand specimen, the section shows that the inner part of the nodule has concentric zones of near circular outline with only slight flattening visible (accurate measurement is not possible as the specimen is partly eroded). 8000a shows similar circular zoning, but as this specimen only extends to a

dark band of the concretion its relationship to the surrounding halo and host rock is unknown. 8000a, f (and c) are also similar in that they contain coarse sandy bands near their cores. Whether there is any formative significance in this, or whether it reflects merely their close proximity in outcrop and/or stratigraphic level is unclear.

Following the initial examination and slicing of the nodules, XRF analysis was undertaken to determine their composition in <sup>s</sup> respect of a suite of elements of particular interest. The results of this analysis helped to guide the detailed investigation of the mineralogy using microprobe and XRD, which was restricted by several factors, including the very fine grain size of some, the difficulty of preparing polished sections of rocks of this type, and availability of instrument time. Microprobe analysis revealed that the elements of interest are mainly concentrated in opaque phases. The most notable exception to this is V, which is widely distributed throughout the nodules, in opaques, and also much of it in the fine brown clayey/micaceous matrix. Some analyses of this material give good mica formulae, but others are apparently mixed phase or amorphous and commonly give very low analytical totals suggesting the presence of unstable, possibly organic material. Subsamples of three nodules with suspected organic component were submitted for analysis by an evolved gas method. This confirmed the presence of abundant carbonate in 8000a but none in 8000f or 8046. Minor amounts of water, attributable to the "clay/mica" (and some to gypsum in 8046) were found, but no detectable organic carbon. (Pyrite was not detected). The nature of the component giving rise to the low totals therefore remains enigmatic.

Most of the opaques are very fine, ranging from sub-micron granules and grain boundary smears to interstitial and subhedral grains or aggregates, rarely exceeding 50  $\mu\text{m}$  diameter. A distinct class of

apparently detrital opaques and near opaques is also found, including sub angular to well rounded grains of ilmenite, Ti oxides, tourmaline and chromite (1 grain in HBR 8010). The majority of opaque grains however, from their form and distribution within the nodules, are considered to have formed in situ. Many of these are compound grains consisting of aggregates of 2 or more phases in varied, often complex textural relationship with each other and with the matrix. These include apparently random irregular intergrowths, crystallographically oriented inclusions and/or exsolution phases, zoned aggregates with cores and rims of radically different phases, and late crack fills, some of these extending into the matrix. In some cases clusters of grains are found with intricate, almost dendritic growths into the matrix. Many of the multiphase opaques are intergrown on a scale at the limits of resolution of the microprobe, ie down to a few  $\mu\text{m}$ . Furthermore, the very small grains do not allow precise quantitative analysis because of uncertainties in the matrix corrections for absorption and fluorescence effects. Some of the analyses therefore may only be regarded as semi-quantitative. The names of the phases apparently present are given, and where appropriate, calculated formulae (tables 6-22). In only a few cases were grains large enough for extraction for XRD identification found. Specimen HBR 8000a, in view of the abundance of opaques and relatively high concentrations of interesting elements, was chosen for bulk analysis by X-ray diffractometry. The trace showed only major quartz, calcite and a mixture of mica/clay phases (broad peaks centred on  $10\text{\AA}$ ,  $4.5\text{\AA}$  and  $2.58\text{\AA}$ ) with minor feldspar and a trace of chlorite. Further work could be undertaken to separate heavy fractions from crushed material to identify the minor phases. More data on those samples studied in detail is given in the following sections.

## Autoradiography

$\alpha$ -track autoradiographs (figure 5) were made from cut surfaces of three specimens showing a range of U values, in order to determine the distribution of U and to attempt to identify uraniferous phases.

HBR 8000a (7100 ppm U). This strongly zoned nodule shows intense but diffuse  $\alpha$ -activity in the central 12mm zone, contrasting sharply with the next zone (1 to 2mm wide) which is almost free of tracks. This "clean" zone corresponds to one of the darkest rings in the nodule, which is rich in sulphide and oxide minerals. Outside this are abundant high intensity spots showing rather less marked concentric zoning. The great abundance of very fine grained opaques in this specimen rendered direct correlation between the autoradiograph tracks and particular grains in the specimen impossible, but during microprobe analysis of the thin section, coffinite (see table 8) was found in composite grains with Co Ni arsenides, and sulphide and oxide minerals in the outer zones of the nodule. In some cases the coffinite occurs apparently as crack infills, but due to the very fine grain and poor polish obtainable this is not certain. Despite the intensity of tracks in the core of the nodule, no definite uraniferous phase was resolved here, but the presence of fine grains or selvages of coffinite is the most likely possibility.

HBR 8000e (1200 ppm U). This ellipsoidal nodule shows a remarkably irregular outline of  $\alpha$ -activity on the autoradiograph, corresponding to a dark, narrow, discontinuous margin with a dendritic appearance suggestive of a diffusion front. The inner part of the nodule shows only some sporadic intense spots with a fine diffuse background. No uraniferous phases were detected, but the dark margin does correspond to concentrations of Co arsenide and Co Ni arsenide minerals, suggesting by analogy with

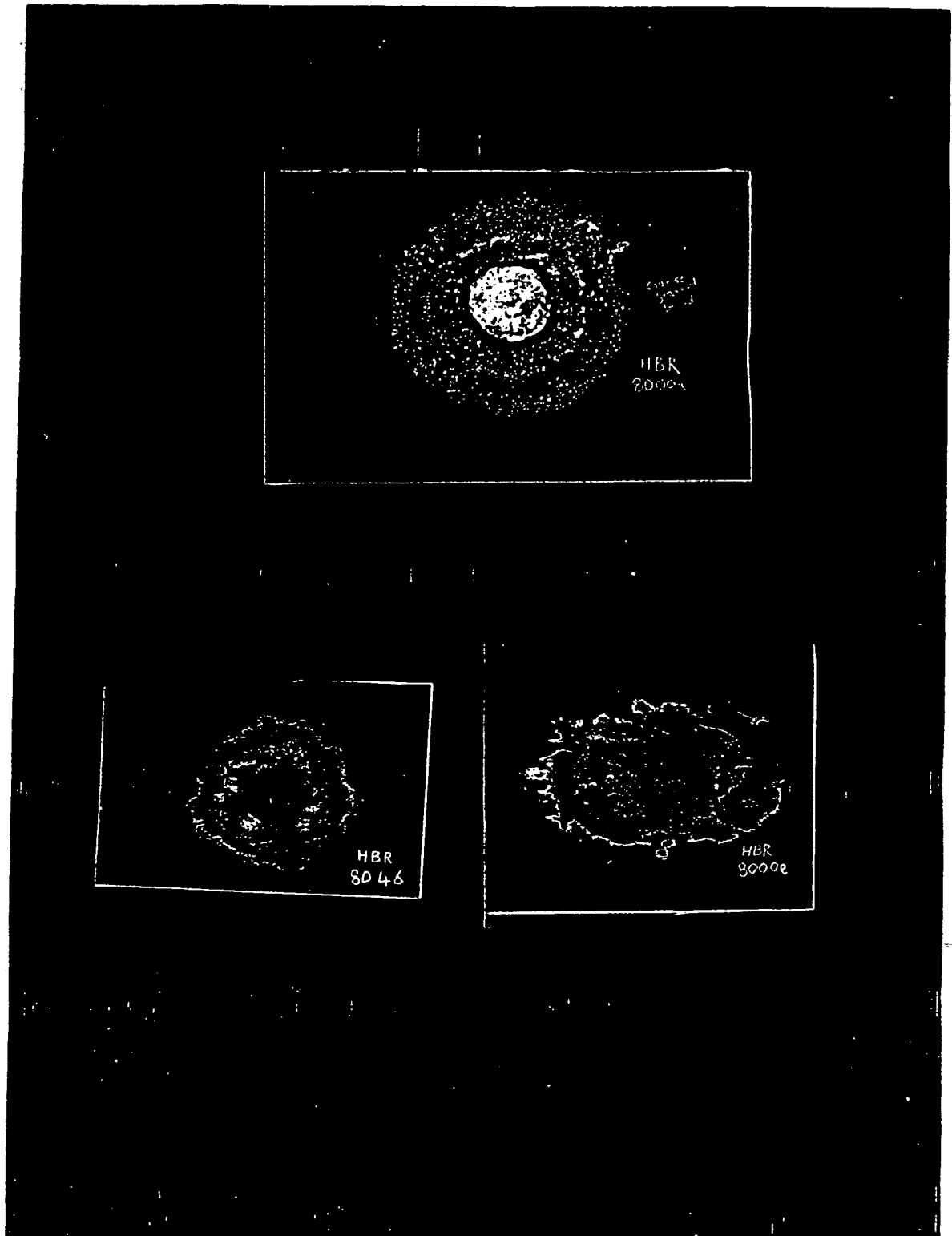


Figure 5. Autoradiographs of nodule slices (x1)

HBR 8000a.	7100 ppm U
8000e	1200 ppm U
8046	80 ppm U

scribed outlines of the cut surfaces shown in red.

8000a, that fine intergrowths of coffinite may be present.

HBR 8046 (80 ppm U). A small, brown (? weathered) nodule with abundant coarse quartz and only very faintly visible zoning. The autoradiograph shows diffuse concentric bands of tracks, with a "front" similar to 8000e. No obviously uraniferous phases were found. Several analyses however, suggest traces of U in the mica or clay matrix, but none approaching the acceptable statistical detection limit for the E.D.S. (about 0.2-0.3 wt % U).

#### Sample notes and results of microprobe analysis

Microprobe analyses were carried out using a Cambridge Instruments Geoscan fitted with Link Systems energy-dispersive X-ray analyser and computer for on-line correction of absorption, fluorescence and atomic number effects. Accelerating voltage was 15kV with a spatial resolution of about 3 to 4  $\mu\text{m}$ . Detection limits vary but are usually about 0.1 to 0.2 wt% element, ranging up to about 0.4 wt% in some combinations where peak overlaps occur in the spectrum. Elements lighter than Na cannot be analysed quantitatively, although F would be detected if present in major amounts. Low analytical totals are therefore obtained from specimens with for example carbonate, water or organic content, and also from some materials which are unstable under electron bombardment. The microprobe cannot distinguish valency states, and this may give rise to uncertainty in the calculation of formulae for minerals containing elements such as V, Mn or Fe, particularly where in combination with undetectable light elements.

Results of analyses are given in tables 6-21. The 'T' numbers are references to the original printout. n.a. = element not analysed; indicates element not detected; tr. = trace probably present; (+) elements

found, not in main list. (included in totals). Total Fe is given as FeO, V as V<sub>2</sub>O<sub>3</sub> or VO(OH). Traces or minor amounts of SiO<sub>2</sub> and elements such as K, Na shown in sulphide analyses are probably due to adjacent unresolved silicate matrix or inclusions. A list of minerals identified (excluding common detrital grains such as zircon, tourmaline, rutile, is given in table 22).

HBR 8000a (tables 6 to 8)

Near spherical nodule with well-marked concentric zones of about 2 to 4mm width, alternating grey and very dark grey, out to about 40mm diameter. The bulk of the nodule is composed of fine sandy calcareous mudstone with a pale greyish brown clay matrix (table 7, T32) with some fine and a little coarse sparry calcite. A 2 to 3mm thick band of coarse sandstone with only a little clay matrix passes through the centre of the nodule. Other more irregular pods and lenticles of sandy sediment also occur. The detrital grains consist largely of poorly sorted rounded to sub-rounded quartz grains with some feldspar and a few lithic fragments, mostly quartzite. Some rounded pellets of mudstone are also present. Minor constituents include mica flakes, apatite, zircon, Ti oxides, and tourmaline (green/brown bicoloured grains). A radiating aggregate of tourmaline with pale greyish blue to bright indigo blue pleochroism is apparently part of a clastic fragment. Opaque grains are very abundant, ranging from about 200  $\mu$ m down to less than 1  $\mu$ m. Many of these are multiphase, and intergrown on a very fine scale, commonly below the resolution of the microprobe. They are more common in the sandy parts of the nodule, mostly interstitial to detrital quartz grains. Some of the larger composite grains are associated with clusters of smaller grains nearby, suggesting some nucleation around, and/or replacement of a component in the original sediment. This possibility is endorsed by

the fact that some grains obviously not entirely detrital (angular and convoluted margins partly enclosing detrital quartz) are nevertheless too large to be merely interstitial. Native Ag for example is found in irregular grains, commonly with mixed phase rims of Cu sulphides and Co/Ni arsenides, some with encrustations or crack fills of coffinite. These phases also occur as individual grains, and composites in combination with black V rich grains (probably montroseite, see table 7). Some opaques rich in Pb and Se probably contain clausthalite.

HBR 8000b (figure 6; tables 9, 10)

Near spherical nodule about 50mm diameter. Mostly silt to fine sand quartz in clay matrix. Some fine carbonate, particularly in the more sandy parts of the nodule, which form irregular lenticles and blobs. No distinct coarse sand beds. A few mica flakes are present and some grains of detrital heavy minerals, mostly Ti-oxides, with some tourmaline and zircon. The nodule has weak concentric zoning of reddish-brown and greyish-brown rings contrasting with a dense opaquerich core about 2½ mm diameter. Outside this core, no mineralisation is apparent, except perhaps for the vanadiferous nature of the clay matrix. (table 10, T46 to 49). The core consists of a translucent greenish yellow Pb, Cu and V rich matrix (table 10 T41 to 45), containing a discontinuous shell of clausthalite (PbSe) about 1mm diameter. (figure 6; table 9, T29 to 31). The matrix within the clausthalite shell and immediately around it consists mostly of a molybdomenite (PbSeO<sub>3</sub>) clausthalite mixture (table 9, T38 to 40); fine particles of clausthalite being contained in a translucent, cloudy mixture of molybdomenite and detrital minerals. Outside this zone, the matrix is still rich in Pb, Cu and V, but lacks Se (above EDS detection limit of about 0.3 wt.% Se). The nature of this material remains uncertain. Se occurs in this outer core as PbSe (clausthalite) particles and coatings on detrital grains (eg T25, table

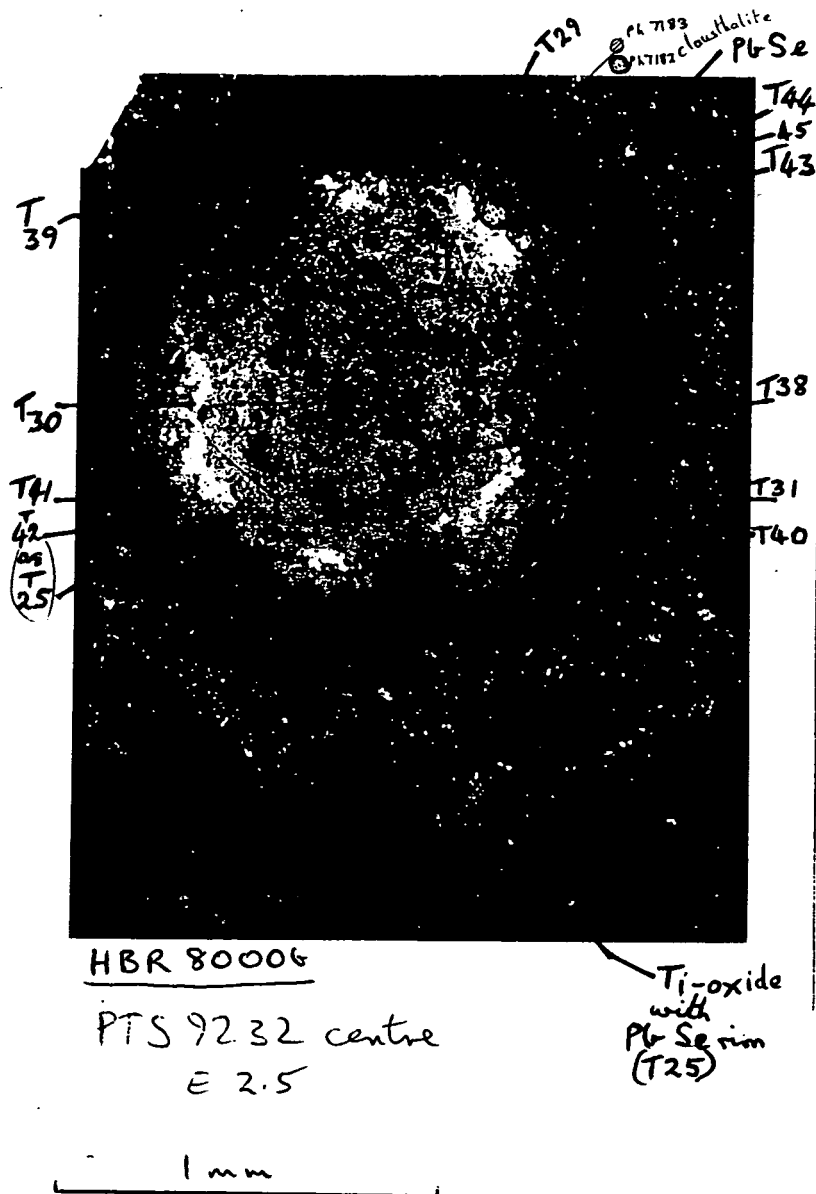


Figure 6. HBR 8000b

clausenthalite-molybdomenite shell at core of nodule (reflected light).

T numbers refer to points analysed see tables 9 and 10.

9 clausenthalite rim on Ti-oxide - see figure 6). The bulk of the nodule (ie outside the  $2\frac{1}{2}$  mm diameter core) contains no detectable Pb, Se or Cu. The molybdomenite in the core probably results from oxidation of the clausenthalite, but the origin of the latter remains obscure.

HBR 8000c - not sectioned. Hand specimen appearance and XRF analysis similar to 8000a.

HBR 8000d - not sectioned

HBR 8000e (tables 11,12)

Flattened ellipsoidal nodule, about 6cm overall maximum diameter, section 40 x 25mm. Silt to fine sand quartz grains in clay matrix. Much angular quartz. Irregular lenticles of silt and medium to fine sand. No distinct core to nodule, or zoning, except for a very irregular narrow dark band near outer margin, corresponding to intense  $\alpha$ -activity shown on autoradiograph (see figure 5). The fine opaques forming this band and in the rest of the section are dominantly Co/Ni arsenides of general formula (Co Ni) As, mostly Co rich, but near-pure niccolite was also found (table 11). Other intermediate values eg (Ni 0.72 Co 0.23)0.95 As were present but no material free enough of impurities to enable good quantitative analysis. The ? modderite (table 11, T13) grain analysed had a rim of more nickeliferous material (table 11, T15). Some (CoNi) As<sub>2</sub> - probably safflorite is also present (table 11, T19). One other analysis gave (Co 0.98 Ni 0.18)1.15 As<sub>2</sub>. Many analyses showed traces of Cu but rarely resolved pure Cu sulphides (eg table 11, T17). The V shown in these analyses is probably present in the V-oxide montroseite which occurs in composite grains with the sulphide/arsenides, and as discrete grains throughout the nodule. (Table 12; T9, 10). V is also abundant in the clay/mica matrix, the highest value shown (T12) being in a coarse mica flake adjacent to a detrital tourmaline grain. Some V is also found in opaque grains showing high Ti + Fe. The composition

of these is very variable, and it seems likely that they are fine mixtures of V oxide with Ti oxides +/- or ilmenite. Despite the strong  $\alpha$ -activity evidenced by the autoradiograph, and the U value shown by XRF, no uraniferous phases were detected.

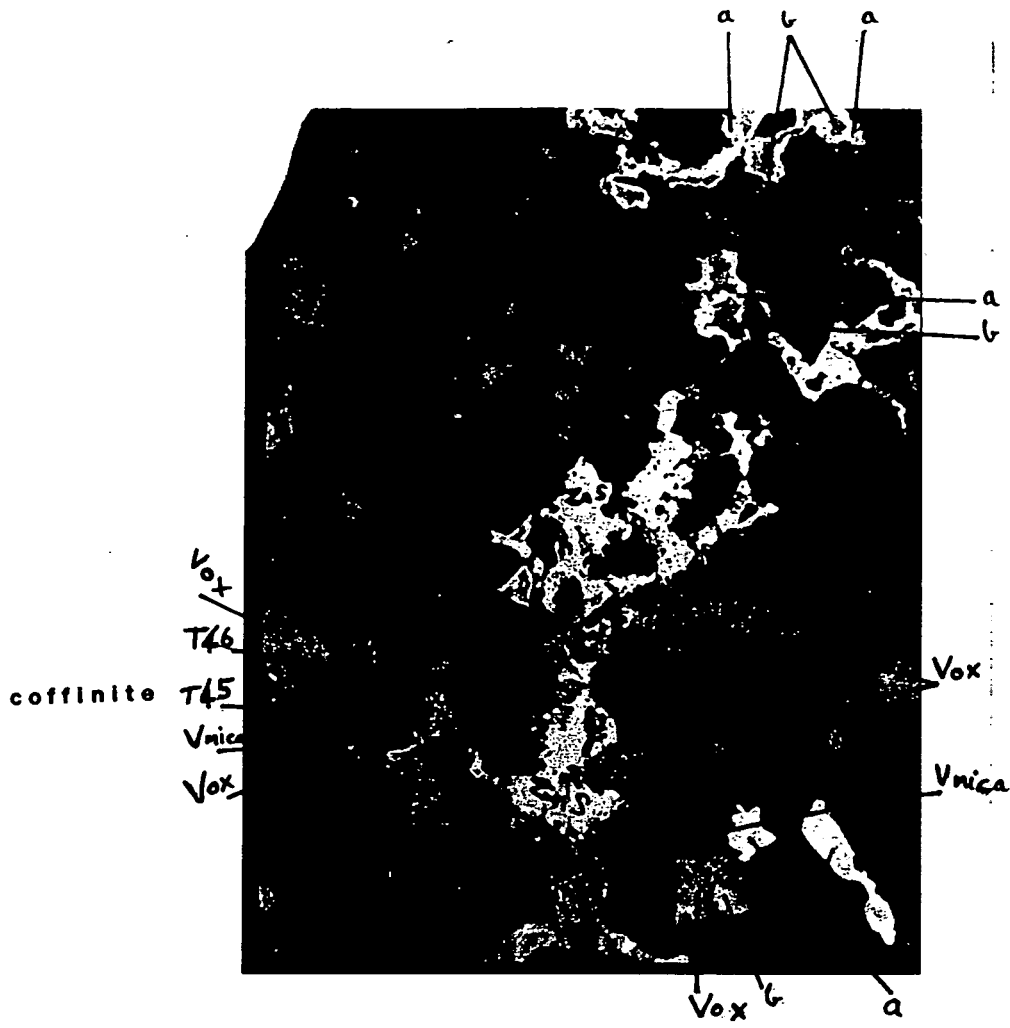
HBR 8000f (figure 7; tables 13 to 17)

Slightly flattened ellipsoidal nodule. Section is 42 x 25mm. The nodule has weak to moderate colour zoning, and near circular outline, with a dark core about 8mm diameter containing abundant opaque grains. The flattening is marked by extension of a dark outer zone to the edges of the nodule along the longer axis of the section, corresponding to a sandy bed 3 to 4mm wide which passes through the centre of the nodule. Other more irregular patches of sandy sediment are also present, contrasting with the bulk of the nodule which is made up of a fine translucent clayey matrix with abundant quartz grains, mostly of silt to fine sand size. Carbonate is present, occurring as sparry calcite cement in the sandy beds. The clayey matrix is highly vanadiferous, and contains some more coarsely crystalline V mica (table 16; T7, 37, 46). A flake of green chlorite also shows a significant V content (table 16; T8).

Opaque phases are abundant throughout the section, particularly near the core, and distributed along the sandy beds. Most are very small, ranging from 0.1mm down to less than 1  $\mu$ m diameter, and rarely exceeding 0.2mm. They commonly form intricate interstitial aggregates and coatings to quartz grains and each other. In figure 6, an example is shown of a field (in a sandy lens) with a particularly varied assemblage, including sulphides of Zn and Cu, V oxide (montroseite), coffinite, and dark brown V-mica. Montroseite was confirmed by XRD (film no Ph7181a) although calculated formulae for VO(OH) from these analyses give high totals (table 16, T57) suggesting that the V oxide phase(s) present do not conform

to this formula. In the absence of other structural or optical data, montroseite is used as a tentative identification for the V-oxide mineral present in these nodules. In figure 6, montroseite appears as mid-grey granular textured material forming equant interstitial grains, intergrowths with sulphides, and plumose aggregates, some forming haloes to detrital quartz grains. (lower right centre). V mica forms much of the matrix in this area, and can be seen forming interstitial masses, and coatings to larger grains such as coffinite (figure 6, left; table 17, T45), and detrital quartz. Two areas of ZnS are seen in figure 6, although this and coffinite are of only minor abundance relative to the V oxide and Cu sulphides in the whole of the section. The ZnS analyses all show minor Cu (eg table 15, T25) possibly due to submicron intergrowth with Cu sulphides. No grains of ZnS were successfully extracted for XRD confirmation of identity.

The Cu sulphides in the section can be classified into 2 broad groups. Table 13 shows Cu sulphides with no other elements detected (apart from minor SiO<sub>2</sub> impurity) which form 2 sub-groups: a) grey reflecting, approx. Cu<sub>1.7</sub>S, and b) blue reflecting approx Cu<sub>1.5</sub>S. Table 14 shows Cu sulphides containing Fe and some minor V and Se. Yellow grains give formulae close to chalcopyrite (T17), whilst blue, purple and grey grains give formulae close to bornite with excess Cu, and in one case (T36) Fe deficiency. In some cases, these compositions can be reconciled with optically resolved intergrowths, inclusions and/or exsolution phases and appropriate mixtures of bornite + chalcopyrite + chalcocite calculated. In others where no visible phase differences are present, such mixtures may be assumed, or the grain considered as non stoichiometric bornite. Figure 6 shows examples of the blue and grey Cu-sulphides occurring as individual grains, and as blue cores with grey rims.



PTS 9235 d  
E 16

0.1 mm

Figure 7 HBR 8000f

Sulphides, coffinite, V mica and montroseite  
(reflected light)

a = grey reflecting Cu-sulphide

b = blue " "

Vox = montroseite

Table 15 shows examples of analyses of phases present as numerous grains, usually tiny (<50 $\mu$ m) and in complex aggregates. These are of minor quantity relative to the V oxide and Cu sulphides, although widely distributed throughout much of the nodule. Several analyses of such material are of multiple mixtures although some give near rational formulae, perhaps fortuitously. eg T49, T54. Ag was found as 2 to 5  $\mu$ m grains of native Ag, commonly associated with clausthalite and in Pb-free seleniferous ? mixtures such as T49, 54.

HBR 8009 not sectioned.

HBR 8010 (figure 8: tables 18, 19)

The specimen consists of a collection of small (8 to 12mm diameter) spherical or slightly flattened nodules. Attempts were made to produce polished thin sections of two of these. The first consists of silt to fine sand quartz in a brown micaceous or clay matrix, with no visible zoning or core. Opaques (detrital?) include Ti oxide with minor Fe and V. Analyses of the matrix show a composition of mica type with variable amounts of V. Examples are shown in table 18, T2 and T3.

Much of the second nodule was lost during sectioning, the remaining portion consisting of a small dark greenish yellow core with concentric zones, surrounded by some sandy clay matrix similar to that of the first example. Analyses of the clay matrix are shown in table 18, T5 and T6. A sketch of the nodule showing the structure of the core and the points of analysis is shown in figure 8. Most of the analyses (table 18; T13, 14; table 19) show enrichment of Pb and Cu in the core, but no S, and only minor Se in some analyses. The totals are also very variable, ranging down to only 40.64% of detectable elements, suggesting the presence of carbonate or organic matter. There are striking similarities between this core, and the core of HBR 8000b, both in form and in the composition of part of the material. The Pb and Cu enriched material without

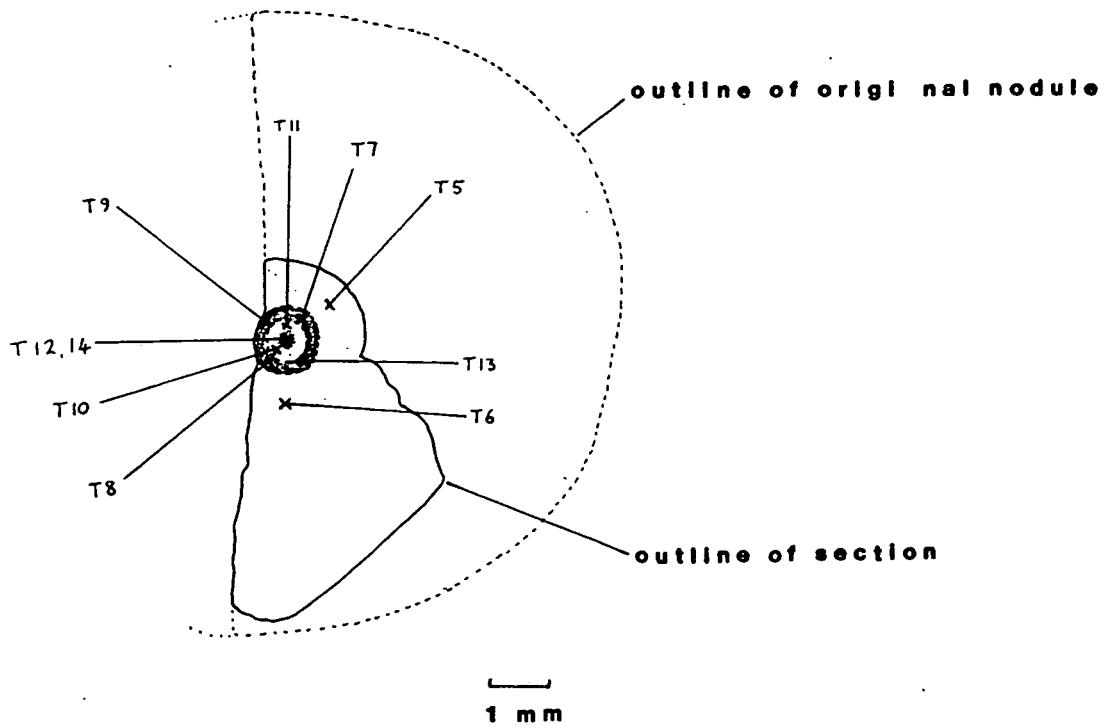


Figure 8 HBR 8010 sketch showing points of analyses (tables 18,19)



Figure 9 HBR 8026 sketch showing structure of nodule

↑ analysed point

significant Se is similar to the translucent material surrounding the clausthalite/molybdomenite core of 8000b. The presence of minor Se in HBR 8010 analyses suggests that some clausthalite and/or molybdomenite might be present.

HBR 8014 not sectioned. - similar to 8026

HBR 8023 not sectioned. grey reduction sphere in marl, with no core, and only low values for XRF analysed elements.

HBR 8026 (only brief analysis undertaken: figure 9)

A small ellipsoidal nodule (20 x 12mm in section) flattened parallel to bedding in silty marl. The nodule consists of dark brown staining in a grey halo in the marl. The radius to the edge of the halo (normal to bedding in section) is 32mm. This boundary between red and grey coloured sediment is sharp to within a few  $\mu\text{m}$ , i.e. the order of size of the finest grains in the sediment, and cross-cuts sedimentary structures such as silt lenticles and fine clay bands. There are very few opaque minerals in the grey part of the nodule, the most prominent being a sparse dendritic structure about 15mm outside the core. The individual particles were too small to resolve, but qualitative analysis of the area showed Mn and Fe above background level for the surrounding sediment. No other significant elements were detected. Analysis of the grey clay matrix outside the central nodule showed major Si, Al, minor K, Mg, Fe and very minor (<1%) Ti, Ca, Na, and Cl. Opaque grains present are Ti oxides, with a few ilmenite and tourmaline. V was not detected.

The central nodule (figure 9) has a weak concentric structure marked in differing shades of brown, with a yellow green staining in the central 2mm zone. The outermost zone is an irregular elliptical ring, but the inner zones are near circular in outline. Only a brief analysis of part of the central zone was made. This gave:

SiO<sub>2</sub> 0.72%; TiO<sub>2</sub> 21.50 %; Al<sub>2</sub>O<sub>3</sub> 0.36%; FeO 6.18%; MgO 1.07%; V<sub>2</sub>O<sub>3</sub> 14.92%; CaO 1.32% K<sub>2</sub>O 0.24%; Na<sub>2</sub>O 0.61%; BaO 1.55%; CuO 12.17%; PbO 35.37%; SeO<sub>3</sub> 1.48%; Cl 0.24%. = total 97.73%.

This Pb-Cu enrichment in the greenish yellow core of an otherwise poorly mineralised nodule shows a strong similarity to HBR 8000b and 8010.

HBR 8045

The section of this nodule shows a dark brown core with concentric rings out to about 12mm diameter. The remainder of the nodule has an even brown colour, suggesting oxidation and probably weathering. The bulk of the nodule is quartz silt in a clay matrix, with silt lenticles. Qualitative microprobe analysis of the darkest brown material in the core showed this to consist largely of V-rich silicate. The structure of this nodule is similar to 8000b, 8010, and 8026. However, very little greenish staining is apparent, and it appears that the slicing has missed the exact centre of the core. In view of these factors, and the XRF data showing only V, Cu and Pb as significantly concentrated in this nodule, no further analyses were undertaken at this stage.

HBR 8046 (tables 20,21)

Near spherical nodule 30mm diameter. Abundant quartz in rounded to well rounded grains up to 1mm diameter. Finer quartz is more angular and passes down into silt grade. A few feldspar grains and some lithic fragments are present. No distinct sedimentary structures are visible, the main variations in the nodule being irregular patches with fewer sand particles in the dark brown clay matrix and a small core (2mm) of very dark brown, near opaque matrix at the centre. Some weak yellow staining is present around this. Only a small quantity of opaque or near-opaque material is present, composed of three types: a) rounded equant or irregular grains, most apparently detrital, including Ti oxide(s), ilmenite and tourmaline. b) grain coatings and irregular patches. c) fine granules in strings and clusters and dispersed in the clay matrix, mostly too small to resolve for microprobe analysis.

Some of the apparently detrital grains have rather unusual compositions, close to Ti oxide or ilmenite, but also showing significant concentrations of V, Cu and Pb, in addition to normal silicate impurities (table 20, T912). These grains occur scattered through the nodule, and are not apparently related to the dark core. The more irregular opaques, commonly forming grain coatings, appear to be composed of very hydrous or possibly organic material, since they give very variable compositions and usually low totals. This material is unusual in this suite of nodules in that it is commonly manganiferous whereas in most of the nodules, only sparse traces of Mn were detected. Examples are shown in table 20, T23 and table 21, T3. Analyses of the clayey matrix in the nodule are also shown in Table 21. This is also very variable; some compositions are close to mica formulae, others are presumably mixtures. Most once again show low totals, an extreme example is T7. The nodule was checked for organic, water, and carbonate content by evolved gas analysis but no significant concentrations were detected. The reason(s) for the low analytical totals therefore remain enigmatic. A consistent feature of this nodule is the presence of V in nearly every point analysed, including some apparently detrital Ti oxide grains. This suggests a pervasive introduction of V, possibly accompanied by some alteration of pre-existing minerals. Significant concentrations of Pb and Cu were also found, particularly in the core (table 21, T5) but no Se, and only very minor amounts of S. Some spectra showed possible traces of U, but none in high enough concentrations for quantitative analysis.

#### Conclusion

The nodules exhibit a wide range of compositions, mineral assemblages and textural features. Only a broad qualitative comparison may be made between them, as each of the specimens is unique in some respects. The present collection shows some similarities to previous material from

the Littleham Cove section but also significant differences. Harrison (1975) found native Cu, Ag, a suite of Co/Ni arsenides and Cu sulphides, coffinite and V mica, but no V oxide or seleniferous phases. He describes annular structures of niccolite-rammelsbergite up to 10mm across, forming cores in grey reduction haloes, and large platy accretions of native Cu up to 160mm diameter, contrasting markedly to the present specimens, none of which contained native Cu, and in which the arsenide phases present are in the form of minute grains scattered through dark grey to brown zoned nodules. Only some of the nodules, from Littleham Cove (HBR 8000 series), were found to contain sulphides, arsenides and V oxide. Those from other localities showed some enrichment of V, mostly in the clay matrix, and some Pb and Cu, present in poorly characterised, probably mixed phase or amorphous material.

Two distinct classes of nodules may therefore be considered:

a) Dark dense nodules with strong colour zoning in the matrix and an obvious geometric centre but no distinct compositional nucleus. These are rich in fine opaques throughout including sulphides, arsenides and V oxide, and some with minor amounts of clausthalite and native Ag. The clay matrix is also highly vanadiferous. This class includes HBR 8000a, e, and f. HBR 8000c and d also appear to belong here, although only on a visual comparison and some inference from XRF analysis.

b) Nodules with a distinct nucleus, usually only a few mm across, commonly enriched in Pb and Cu + Se, outside which colour zoning is visible, but little mineralisation is evident, apart from V enrichment. This includes HBR 8000b, 8010 (part), 8026 and 8045. (8014 appears very similar to 8026).

HBR 8009 and 8046 fall outside a rigid application of these categories, but appear closer to type b) than a). 8023 is a grey sphere with no core, and is similar in appearance to the outer zones of 8014 and 8026.

It is apparent that further work might be undertaken to characterise these structures more fully. Examination of more samples may indicate whether the above division is real, or an artefact of sampling, with gradations between the types described. If such a division is real, then its relationship to the field occurrence of the nodules vis a vis stratigraphic horizon or proximity to structural features may be significant. The degree of weathering might also be a factor in the differences, those nodules carrying sulphides, arsenides and V oxides being harder and generally darker than those without.

Further work could also include other techniques not yet attempted such as analytical SEM to enable larger areas to be elementally mapped than is possible with the microprobe. Careful crushing and/or solution of material and heavy mineral extraction might enable concentration of some of the phases for confirmation by XRD.

#### Acknowledgments

XRF analysis was carried out by D.J. Bland, evolved gas analysis by A.J. Bloodworth. Polished thin sections were prepared by G.R. Brumby and C.W. Wheatley.

#### References

Harrison, R.K. 1975. "Concretionary concentrations of the rarer elements in Permo-Triassic Red Beds of Southwest England". Bulletin Geol. Surv. G.B. No52.

Table 6. HBR 8000a microprobe analyses: Sulphides

wt.%	T3	T8	T14	T15	T16	T34	T35
Co	-	0.43	0.33	-	0.92	1.38	0.73
Ni	-	0.57	-	-	3.88	2.79	7.31
Cu	2.34	73.89	76.33	79.56	25.67	49.18	59.51
Ag	95.95	1.46	2.63	1.25	49.52	10.05	1.85
V	-	0.31	0.26	0.31	-	0.83	-
Fe	-	0.41	-	-	-	-	0.46
As	-	1.53	tr.	tr.	11.16	12.21	11.46
S	0.40	19.66	19.65	20.35	9.13	13.80	16.13
SiO <sub>2</sub>	0.41	1.11	0.48	0.32	0.51	3.16	1.16
	<u>99.10</u>	<u>99.37</u>	<u>99.68</u>	<u>101.79</u>	<u>101.10</u>	<u>94.75</u>	<u>100.32</u>

(+) Se tr.

Cl 0.31

Al<sub>2</sub>O<sub>3</sub> 0.71

Al<sub>2</sub>O<sub>3</sub> 0.56

Se 0.64

UO<sub>2</sub> 1.15

Se tr.

T3 native Ag

T8 chalcocite-digenite Cu<sub>1.90</sub>S ; +? langisite (Co<sub>0.35</sub> Ni<sub>0.48</sub>)<sub>0.83</sub> As

T14 ? djurleite Cu<sub>1.96</sub>S;+Ag

T15 ? djurleite Cu<sub>1.97</sub>S;+Ag

T16 mixture Cu<sub>1.42</sub>S;+Ag;+ rammelsbergite (Co<sub>0.21</sub> Ni<sub>0.89</sub>)<sub>1.09</sub> As<sub>2</sub>

T34 mixture including probable chalcocite-digenite + Ag.

T35 chalcocite-digenite Cu<sub>1.86</sub>S;+ niccolite (Co<sub>0.08</sub> Ni<sub>0.87</sub>)<sub>0.96</sub> As

native Ag confirmed by XRD - film no. Ph 7178

Table 7. HBR 8000a microprobe analyses: montroseite, chlorite

wt. %	T7	T10	T12	T17	T22	T32
SiO <sub>2</sub>	1.19	0.96	0.71	1.30	23.70	31.41
TiO <sub>2</sub>	-	0.26	0.39	0.25	-	4.60
Al <sub>2</sub> O <sub>3</sub>	1.53	1.64	1.30	1.89	22.41	13.14
FeO	-	0.38	-	-	29.23	1.05
MgO	*	0.34	0.61	0.54	9.04	2.32
MnO	-	n.a.	n.a.	n.a.	0.25	-
CaO	0.55	0.54	0.31	0.38	-	0.50
K <sub>2</sub> O	0.56	0.12	-	0.40	0.23	5.31
Na <sub>2</sub> O	*	n.a.	n.a.	n.a.	0.27	0.39
V <sub>2</sub> O <sub>3</sub>	89.57	81.89	75.76	92.96	0.72	5.89
Cl	n.a.	tr.	0.30	n.a.	n.a.	0.18
SO <sub>3</sub>	-	tr.	0.31	n.a.	n.a.	0.27
Cu	-	tr.	-	-	n.a.	n.a.
	<u>93.40</u>	<u>83.16</u>	<u>79.69</u>	<u>98.22</u>	<u>85.85</u>	<u>65.06</u>

(+) As tr.

As 0.50

\* = minor amount present, not quantitatively analysed.

T7	? montroseite <sup>x</sup>	V as VO(OH)	100.32
T10	"	"	91.73
T12	"	"	84.85
T17 ??	"	"	104.13

T22 brown chlorite	Si	5.238	)	<u>8.00</u>	)	
	Al	2.762	)		)	
	Al	3.000	)		)	
	Fe(as2+)	5.401	)		)	to 28 oxygen
	Mg	2.976	)		)	
	Mn	0.048	)	11.733	)	
	V	0.126	)		)	
	K	0.067	)		)	
	Na	0.115	)		)	

T32 "clay" matrix + ? carbonate; + ?? organic matter

<sup>x</sup> (monteroseite confirmed by XRD in HBR 8000f)

Table 8 HBR 8000a microprobe analyses: coffinite

wt.%	T21	T23
SiO <sub>2</sub>	11.24	21.05
Al <sub>2</sub> O <sub>3</sub>	0.53	4.52
FeO	-	1.23
MgO	-	1.50
CaO	1.72	0.71
K <sub>2</sub> O	0.42	2.20
Na <sub>2</sub> O	0.48	-
UO <sub>2</sub>	65.78	42.48
Y <sub>2</sub> O <sub>3</sub>	2.85	2.41
P <sub>2</sub> O <sub>5</sub>	0.61	0.41
CuO	-	3.62
PbO	-	1.68
V <sub>2</sub> O <sub>3</sub>	1.37	4.79
As <sub>2</sub> O <sub>5</sub>	1.47	0.72
SeO <sub>3</sub>	0.55	0.71
SO <sub>3</sub>	0.39	1.56
Cl	-	0.12
	<hr/>	<hr/>
	87.41	89.71
	<hr/>	<hr/>

Table 9 HBR 8000b microprobe analyses: clausthalite, molybdomenite

wt.%	T25	T29	T30	T31	T38	T39	T40
Pb	64.81	69.98	68.77	70.86	60.15	59.77	54.51
Cu	4.09	-	0.62	0.66	1.32	2.32	4.39
Se	25.94	26.21	25.98	29.34	21.49	20.66	25.43
S	0.86	-	-	-	-	-	-
SiO <sub>2</sub>	1.18	n.a.	n.a.	-	0.36	-	0.74
TiO <sub>2</sub>	0.66	n.a.	n.a.	-	-	-	-
Al <sub>2</sub> O <sub>3</sub>	0.62	n.a.	n.a.	-	-	-	0.97
V <sub>2</sub> O <sub>3</sub>	1.75	-	-	-	1.64	2.80	-
MgO	n.a.	n.a.	n.a.	n.a.	-	0.69	0.77
CaO	0.40	n.a.	n.a.	-	-	-	-
K <sub>2</sub> O	0.17	n.a.	n.a.	-	-	-	-
Cl	0.35	n.a.	n.a.	tr.	0.18	0.40	0.19
	<u>100.83</u>	<u>96.19</u>	<u>95.37</u>	<u>100.36</u>	<u>85.14</u>	<u>86.64</u>	<u>87.00</u>

T25 clausthalite(Pb<sub>0.95</sub>?Cu<sub>0.05</sub>) Se, + Cu<sub>1.81</sub>S; or  
(Pb<sub>0.88</sub> Cu<sub>0.18</sub>)<sub>1.06</sub> (Se<sub>0.92</sub>S<sub>0.08</sub>). (+ matrix)

T29 " Pb<sub>1.02</sub> Se - confirmed XRD - film no. Ph 7182

T30 " (Pb<sub>1.01</sub> Cu<sub>0.03</sub>)<sub>1.04</sub> Se

T31 " (Pb<sub>0.92</sub> Cu<sub>0.03</sub>)<sub>0.95</sub> Se

T38-40 clausthalite-molybdomenite (Pb SeO<sub>3</sub>) mixtures  
presence of molybdomenite confirmed by XRD - film no. Ph 7183

Table 10. HBR 8000 b microprobe analyses: silicate matrix.

wt.%	T41	T42	T43	T44	T45	T46	T47	T48	T49
SiO <sub>2</sub>	24.42	13.85	31.99	34.47	39.94	45.50	30.17	48.40	46.25
TiO <sub>2</sub>	0.55	-	-	0.39	0.87	0.32	-	0.55	0.30
Al <sub>2</sub> O <sub>3</sub>	16.18	9.69	14.26	15.79	14.84	20.34	18.03	22.72	17.42
FeO	2.75	0.62	1.16	1.82	1.40	1.93	19.27	2.05	0.83
MgO	2.33	0.80	2.40	2.42	3.06	3.70	5.95	3.36	2.39
CaO	1.18	1.92	0.92	0.99	0.99	0.26	0.25	0.52	-
K <sub>2</sub> O	4.28	3.00	5.03	5.73	5.56	7.70	1.81	7.52	5.72
Na <sub>2</sub> O	0.91	0.77	0.56	0.41	0.51	0.40	0.71	0.67	0.34
V <sub>2</sub> O <sub>3</sub>	13.12	14.38	11.15	7.70	8.48	5.31	1.91	8.21	2.83
CuO	10.56	13.50	7.75	2.89	3.48	-	0.52	-	-
PbO	21.08	13.53	3.80	5.72	6.55	-	-	-	-
Cl	-	0.40	0.30	0.42	0.20	0.15	0.17	-	0.34
	<u>98.94</u>	<u>77.89</u>	<u>82.46</u>	<u>78.75</u>	<u>86.25</u>	<u>85.61</u>	<u>80.32</u>	<u>94.49</u>	<u>77.17</u>

(+) BaO 1.58 BaO 5.43 BaO 3.66 SO<sub>3</sub> 0.37 MnO 0.57 SO<sub>3</sub> 0.49 ZnO 0.51  
 ZnO 0.96 SO<sub>3</sub> 0.24

T41 - 49 Se analysed, not detected

T41 - 45 translucent material around Pb/Se rich core (41-44 yellow-green  
 45 - brown)

T46 brown clay matrix; 3mm from centre

T47 green chlorite; 6mm from centre

T48 dark red-brown clay matrix; 24mm from centre

T49 pale brown clay m.; 20mm from centre

ionic formulae

T46 (22 Oxygen) (K,Na,Ca = 1.623) (Al,Mg,Fe,Ti,V = 4.092) (Si+Al = 8)

T47 (28 Oxygen) (Si+Al = 8) (res. Al + other cats. = 10.894)

T48 (22 Oxygen) (K,Na,Ca, = 1.553) (Al,Mg,Fe,Ti,V = 4.063) (Si + Al = 8)



Table 12. HBR 8000e microprobe analyses: montroseite, clay matrix

wt.%	T9	T10	T11	T12	T22	T23	T24
SiO <sub>2</sub>	1.77	2.02	40.56	46.64	48.12	49.03	45.70
TiO <sub>2</sub>	0.42	-	0.22	-	0.22	0.40	-
Al <sub>2</sub> O <sub>3</sub>	1.29	1.35	15.77	7.55	21.33	18.31	11.20
FeO	0.33	0.41	5.82	0.43	2.52	2.13	0.37
MgO	0.68	0.50	3.33	2.60	2.83	2.76	1.81
V <sub>2</sub> O <sub>3</sub>	82.84	85.88	9.65	29.09	8.76	10.99	26.74
CaO	0.98	0.81	1.11	1.67	0.45	0.51	0.55
K <sub>2</sub> O	0.33	0.40	6.50	3.66	7.71	7.74	4.87
Na <sub>2</sub> O	0.38	0.34	0.47	0.30	0.67	0.37	-
SO <sub>3</sub>	0.27	0.71	1.52	0.68	0.27	0.36	0.54
Cl	0.13	-	0.14	-	0.10	-	-
	<u>90.25</u>	<u>92.42</u>	<u>85.48</u>	<u>92.62</u>	<u>92.98</u>	<u>92.60</u>	<u>91.78</u>

(+) PbO 0.83

PbO 0.39

T9 ? montroseite V as VO(OH) = 92.79 ; total 100.20

T10 ? " " = 96.20 ; total 102.74

T11, 12, 22, 23, 24 - "mica/clay" matrix

ionic formulae

	T11	T12	T22	T23	T24
K Na Ca	1.616	1.019	1.618	1.561	1.031
Al Fe Mg V Ti	3.965	4.040	4.087	4.014	4.100
Si Al	8	8	8	8	8
To 22 Oxygen					

Table 13. HBR 8000f microprobe analyses: ? chalcocite-digenite

wt. %	T3	T5	T18	T29	T30	T39	T42
Cu	76.19	77.28	75.44	74.45	75.36	72.98	74.38
S	22.27	22.57	22.45	24.32	22.71	24.94	23.60
SiO <sub>2</sub>	0.71	1.03	0.94	tr	0.53	0.36	0.58
	99.17	100.88	99.19	99.07	98.60	98.71	99.21
(+)			V 0.36	Se 0.3		V 0.43	V 0.25 Ag 0.4
ionic Cu/S	1.74	1.74	1.71	1.54	1.68	1.47	1.58
colour	*	grey	grey	blue	lightgrey	blue	*

The colours shown may be affected by C-coating for microprobe analysis.

\* colour of these grains not recorded.

Table 14. HBR 8000f chalcopyrite (T17), +probable bornite/chalcopyrite/  
chalcocite mixtures

wt.%	T6	T10	T17	T34	T36	T15
Cu	58.83	61.14	31.85	61.01	68.71	55.68
Fe	9.17	9.50	25.92	9.18	5.29	8.28
V	0.77	0.18	n.a.	-	-	1.05
S	26.21	27.11	36.20	26.97	26.23	25.98
Se	0.31	-	0.31	-	-	0.36
SiO <sub>2</sub>	0.96	0.53	n.a.	0.39	-	0.51
	<hr/> 97.05 <hr/>	<hr/> 98.46 <hr/>	<hr/> 94.28 <hr/>	<hr/> 97.55 <hr/>	<hr/> 100.23 <hr/>	<hr/> 92.16 <hr/>
(+)	Pb 0.80					
<u>ionic</u>						
Cu	5.67	5.65	0.88	5.70	5.28	5.45
Fe	0.98	1.00	0.82	0.95	0.44	0.95
S	5.00	5.00	2.00	5.00	4.00	5.00
Colour	*	blue	yellow	purple	brightblue	grey

The colours shown may be affected by C-coating for microprobe analysis.

\* colour of these grains not recorded.

Table 15. HBR 8000f microprobe analyses: sulphides, arsenides, selenides

wt.%	T22	T23	T24	T25	T28	T43	T47	T49	T52	T54
Fe	-	-	-	-	-	0.36	-	-	-	-
Co	16.33	15.73	16.99	n.a.	tr.	-	n.a.	1.73	-	-
Ni	12.08	13.50	12.08	n.a.	-	n.a.	n.a.	n.a.	n.a.	-
Cu	2.69	1.87	1.28	2.92	14.41	38.46	1.55	56.94	-	9.34
Zn	-	-	n.a.	63.87	2.22	-	n.a.	n.a.	2.10	-
V	-	-	-	0.54	-	3.18	0.36	0.27	0.54	0.31
Ag	n.a.	n.a.	n.a.	n.a.	tr.	-	n.a.	1.23	-	62.68
Pb	-	-	-	n.a.	59.45	27.65	69.68	-	78.63	-
As	70.21	70.59	71.57	n.a.	n.a.	-	n.a.	13.98	0.28	0.54
S	0.77	0.41	0.30	32.03	3.50	11.51	0.70	20.10	12.17	1.50
Se	-	-	-	0.63	23.93	12.96	24.56	2.90	0.28	26.93
SiO <sub>2</sub>	0.47	-	0.39	1.28	-	n.a.	n.a.	1.11	1.50	0.47
	103.13	102.10	102.61	102.06	103.51	96.37	97.53	99.17	96.46	101.77

(+) CaO 0.17  
Sb 0.41  
Cd 0.79  
Al tr.  
K tr.  
TiO<sub>2</sub> 1.75  
CaO 0.27  
Cl 0.23  
Cd 0.44  
Sb 0.43  
K<sub>2</sub>O 0.41  
CaO 0.48  
Al<sub>2</sub>O<sub>3</sub> 0.55

T22,23,24 safflorite-rammelsbergite or Ni skutterudite ; + minor "chalcocite"

T22 (Co<sub>0.59</sub> Ni<sub>0.44</sub>)<sub>1.03</sub> As<sub>2</sub>; T23 (Co<sub>0.57</sub> Ni<sub>0.49</sub>)<sub>1.05</sub> As<sub>2</sub>; T24 (Co<sub>0.60</sub> Ni<sub>0.43</sub>)<sub>1.03</sub> As<sub>2</sub>

T25 ZnS ? sphalerite or wurtzite

T28 clausthalite + chalcocite Pb<sub>0.95</sub>Se ; Cu<sub>2.08</sub>S

T43 " " /digenite + impurities.

T47 " + tr. covellite? Pb<sub>1.08</sub>Se ; Cu<sub>1.09</sub>S

T49 Cu<sub>4.00</sub> (As<sub>.835</sub>Se<sub>.165</sub>)<sub>1</sub> S<sub>2.80</sub> unidentified phase(s)/? mixture.

T52 galena + impurities.

T54 mixture; including ? nat. Ag +/- or Ag Cu Se S phase ( Ag/Cu = 3.95/1  
( Ag/Se+S = 2.99/2  
( Cu/Se+S = 3.03/8  
( Cu<sub>3.03</sub> Ag<sub>11.97</sub> Se<sub>7.03</sub> S<sub>0.97</sub>

Table 16. HBR 8000f microprobe analyses: V oxide, micas, chlorite

wt.%	T2	T20	T26	T38	T57	T7	T37	T46	T8
SiO <sub>2</sub>	0.37	0.56	0.44	0.64	0.43	36.31	47.81	44.31	26.63
TiO <sub>2</sub>	0.23	-	-	-	-	-	0.99	-	-
Al <sub>2</sub> O <sub>3</sub>	1.17	1.52	0.93	1.53	1.64	8.43	16.05	14.79	19.69
FeO	-	-	-	-	-	0.28	0.56	2.85	17.67
MgO	0.52	0.53	0.45	0.60	0.81	2.36	2.65	3.10	9.64
MnO	-	-	-	-	-	-	-	0.33	0.87
V <sub>2</sub> O <sub>3</sub>	99.64	99.01	99.50	97.04	96.05	22.82	19.15	18.32	2.53
CaO	0.60	1.08	0.47	0.64	0.82	5.79	1.15	0.88	0.46
K <sub>2</sub> O	0.21	0.16	0.26	0.19	0.13	6.84	8.82	7.51	0.62
Na <sub>2</sub> O	-	-	-	0.37	0.38	0.25	tr	0.79	0.48
SO <sub>3</sub>	n.a.	n.a.	n.a.	n.a.	n.a.	0.42	0.29	-	-
P <sub>2</sub> O <sub>5</sub>	n.a.	n.a.	n.a.	n.a.	n.a.	3.00	0.30	n.a.	-
Cl	n.a.	n.a.	n.a.	n.a.	n.a.	0.23	n.a.	n.a.	0.09
	102.74	102.86	102.05	101.01	100.26	86.73	97.77	92.88	78.68

T2, 20, 26, 38, 57: V - oxide ? montroseite eg T57 V as VO(OH) = 107.58

T7 V-rich clay matrix

T8 Chlorite (Si+Al)<sub>8</sub> (r. Al + other cats.)<sub>11.152</sub> (Oxygen<sub>28</sub>)

T37 V-mica (Si+Al)<sub>8</sub> (K Na Ca)<sub>1.756</sub> (r. Al+Y cats.)<sub>3.871</sub> (Oxygen<sub>22</sub>)

T46 V-mica (Si+Al)<sub>8</sub> (K Na Ca)<sub>1.748</sub> (r. Al+Y cats.)<sub>4.141</sub> (Oxygen<sub>22</sub>)

(T46 adjacent coffinite T45)

Table 17. HBR 8000f microprobe analyses: coffinite.

wt.%	T4	T45	T55
SiO <sub>2</sub>	37.90	18.33	7.32
Al <sub>2</sub> O <sub>3</sub>	0.59	1.68	0.93
FeO	-	0.37	-
MgO	0.33	0.35	-
V <sub>2</sub> O <sub>3</sub>	1.15	1.58	1.03
CaO	1.18	1.51	1.36
K <sub>2</sub> O	0.45	0.46	-
Na <sub>2</sub> O	0.98	0.86	0.92
UO <sub>2</sub>	45.71	55.31	69.28
Y <sub>2</sub> O <sub>3</sub>	2.72	5.07	1.75
P <sub>2</sub> O <sub>5</sub>	1.01	1.96	1.13
CuO	2.99	-	n.a.
As <sub>2</sub> O <sub>5</sub>	n.a.	-	2.58
SO <sub>3</sub>	n.a.	-	0.66
Cl	n.a.	n.a.	0.16
	<u>95.01</u>	<u>87.48</u>	<u>87.12</u>

Table 18. HBR 8010 microprobe analyses; V mica, clay matrix

wt%	T2	T3	T5	T6	T13	T14
SiO <sub>2</sub>	57.30	45.82	48.16	49.64	41.06	16.76
Al <sub>2</sub> O <sub>3</sub>	17.40	17.90	10.56	21.38	16.99	4.91
FeO	4.15	0.48	0.69	2.18	2.31	1.00
MgO	3.40	1.85	2.58	3.02	2.81	1.24
V <sub>2</sub> O <sub>3</sub>	7.76	18.20	24.43	10.61	13.56	4.82
CaO	0.53	0.87	2.83	0.63	0.80	0.37
K <sub>2</sub> O	6.36	5.62	3.38	8.23	6.36	1.99
Na <sub>2</sub> O	0.34	-	0.25	0.29	0.50	0.42
CuO	n.a.	n.a.	-	-	2.29	1.58
PbO	n.a.	n.a.	-	-	6.83	7.01
	<hr/> 97.60 <hr/>	<hr/> 90.74 <hr/>	<hr/> 93.13 <hr/>	<hr/> 95.98 <hr/>	<hr/> 93.51 <hr/>	<hr/> 40.64 <hr/>

(+) TiO<sub>2</sub> 0.36 SO<sub>3</sub> 0.25 Cl 0.54

T2 nodule a, brown clay matrix

T3 nodule a, brown micaceous matrix

T5,6 nodule b, brown clay matrix outside core

T13,14, nodule b, brown clay matrix in core.

ionic formulae

	T2	T3	T5	T6	T13	T14
K Na Ca	1.221	1.214	1.107	1.590	1.502	1.409
Al Fe Mg V Ti	4.103	4.172	3.987	4.104	3.796	2.952
Si Al	8	8	8	8	8	8
Oxygen	22	22	22	22	22	22

Table 19. HBR 8010 microprobe analyses: dark matrix at core of nodule

wt.%	T7	T8	T9	T10	T11	T12
SiO <sub>2</sub>	1.31	8.89	6.77	1.34	2.10	1.10
TiO <sub>2</sub>	-	0.42	0.99	-	-	-
Al <sub>2</sub> O <sub>3</sub>	0.63	3.90	3.15	0.84	0.95	0.51
FeO	0.39	0.50	0.99	-	0.48	-
MgO	0.31	0.93	0.84	0.50	0.58	0.37
V <sub>2</sub> O <sub>3</sub>	12.69	18.07	14.58	13.12	19.18	13.98
CaO	0.48	0.45	0.41	1.16	0.67	0.54
K <sub>2</sub> O	0.22	1.72	1.13	0.17	0.17	-
Na <sub>2</sub> O	0.43	0.64	0.89	0.50	1.08	0.83
CuO	10.16	13.29	10.71	10.89	17.60	11.52
PbO	36.98	43.99	37.55	33.69	53.05	39.37
SeO <sub>3</sub>	0.86	-	-	-	2.70	1.02
Cl	0.38	0.25	0.47	0.38	0.19	0.30
	<u>64.84</u>	<u>93.05</u>	<u>78.48</u>	<u>62.59</u>	<u>98.75</u>	<u>69.54</u>

probably mixtures of oxides + ? carbonate + ? organic matter.

Table 20. HBR 8046 microprobe analysis: opaque grains

wt. %	T9	T10	T11	T12	T23	T24
SiO <sub>2</sub>	0.48	0.47	10.00	1.72	0.25	34.89
TiO <sub>2</sub>	40.80	72.87	66.19	78.50	-	-
Al <sub>2</sub> O <sub>3</sub>	0.43	0.27	5.80	0.83	-	10.31
FeO	23.57	9.61	2.52	5.75	0.62	3.85
MgO	0.23	-	0.95	0.30	0.37	2.66
V <sub>2</sub> O <sub>3</sub> *	5.9	5.4	4.3	6.1	0.35	13.36
CaO	0.43	0.45	0.61	0.51	1.17	1.26
K <sub>2</sub> O	-	-	1.47	0.26	-	4.71
Na <sub>2</sub> O	0.26	-	0.46	0.30	-	0.55
PbO	6.47	8.06	4.53	5.79	0.83	-
CuO	2.15	3.32	1.62	1.66	-	0.63
	<u>83.21</u>	<u>100.45</u>	<u>98.45</u>	<u>101.72</u>	<u>29.09</u>	<u>75.30</u>

(+)	MnO 2.31	MnO 23.70	ZnO 0.56
	BaO ?tr.	SO <sub>3</sub> 0.37	SO <sub>3</sub> 0.77
	Cl 0.19	Cl 0.44	Cl 0.35
		BaO 0.99	P <sub>2</sub> O <sub>5</sub> 0.5
			Y <sub>2</sub> O <sub>3</sub> 0.9

\*Values for minor V in presence of major Ti are less precise due to peak overlap in spectrum.

T9 mixture ? mostly ilmenite  
 T10-12 impure "Ti-oxides": phase not determined.  
 T23 Mn-rich op with v. low total. ? organic +/- polyhydrate.  
 T24 dark brown near-opaque matrix to T23.

Table 21. HBR 8046 microprobe analyses: micas + mixed fine matrix

wt. %	T3	T5	T6	T7	T4	T19	T20	T21	T22
SiO <sub>2</sub>	21.00	9.73	27.06	10.82	43.08	47.04	42.29	29.08	45.52
TiO <sub>2</sub>	-	-	-	-	0.32	0.42	0.66	-	-
Al <sub>2</sub> O <sub>3</sub>	8.56	2.53	9.21	3.11	16.32	22.26	16.53	9.74	9.52
FeO	3.45	1.84	1.33	0.42	2.46	3.71	1.21	1.88	2.98
MgO	1.48	0.93	1.38	0.73	2.60	2.81	2.32	1.17	2.89
V <sub>2</sub> O <sub>3</sub>	3.01	13.27	4.62	3.07	11.21	5.68	9.66	13.28	21.55
CaO	1.40	1.78	0.31	0.32	0.40	0.47	0.47	0.69	2.09
K <sub>2</sub> O	2.89	0.82	3.70	0.74	7.56	9.27	6.73	2.66	2.84
Na <sub>2</sub> O	0.22	0.46	0.36	0.33	0.32	0.37	0.56	-	-
CuO	0.42	6.32	0.60	-	-	-	0.84	0.75	0.67
PbO	-	18.57	1.76	-	-	n.a.	1.33	1.72	-
SO <sub>3</sub>	-	-	-	0.17	0.31	-	0.55	0.67	0.63
Cl	0.23	0.39	0.34	0.66	-	-	0.23	0.38	-
	59.22	56.64	50.67	20.37	84.58	92.03	83.38	62.59	88.69

(+) MnO 15.83  
BaO 0.73

ZnO 0.57

T3, 5, 6, 7 translucent dark red to brown matrix + encrusting material mixtures: all give v. low totals. ? organic matter +/- carbonate. 5, 6, and 7 are in the dark core zone; 3 is encrustation on quartz grain near margin of the nodule.

T 4, 19, 20, 22 - brown clayey/micaceous matrix; outside core.

T21 - red translucent matrix outside core.

<u>ionic formulae</u>	T4	T19	T20	T22	T21
K Na Ca	1.663	1.869	1.611	0.878	0.901
Ti Al Fe Mg V	4.057	4.158	3.792	4.108	3.886
Si Al	8	8	8	8	8
Oxygen	22	22	22	22	22

some spectra suggest traces of U, but not detected in quantitative analyses

Table 22. minerals identified (excluding common detrital grains)

HBR	8000a	8000b	8000e	8000f	8010	8046	Other
V-mica	/	/	/	/	/	/	
montroseite	/		/	X			
chlorite	X		/	/			
calcite	/			/			
coffinite	/			/			
chalcocite/	/	?	/	/			
digenite							
djurleite	/						
covellite?				?			
bornite?				?			
chalcopyrite				/			
pyrite				/			
galena				/			
sphalerite?				/			
native Ag	X			/			
niccolite	/		/				
modderite			/				
langisite	/		/				
safflorite/							
rammelsbergite/	/		/	/			
skutterudite/							
metadomeykite							X
clausthalite	/	X		/			
molybdomenite		X		?			

/ probably present (identified by probe analysis)

X confirmed by XRD

? uncertain (occurs as very fine mixtures or polymorphous compounds. e.g. Zns may be sphalerite or wurtzite)

## Appendix to Mineralogical Report 85/12

### XRF results for vanadium-bearing nodules

The results are given in four tables (1-4), the first containing the majority of the semiquantitative information, the second containing the details of the other elements detected (semiquantitative data where available) whilst the third contains the semiquantitative ( $\sim 10\%$  relative error) "whole rock" elements. In table 3, HBR8000b was analysed on a cut slice and the results are about 20% high since the calibration is based on samples diluted by 20% elvacite. The  $\text{Cr}_2\text{O}_3$  results have not been corrected for the overlap of vanadium and are thus too high.

The data from the first table was used to obtain some statistical information (table 4), and the pairs giving highly significant correlations were plotted as figures 1 to 4.

An additional nodule was available (collected from the cliff at Littleham Cove) and was examined in a more destructive fashion. Portions of the nodule seen to contain a silvery white phase on the cut surface, were gently crushed and an attempt made to disrupt the nodule by immersion in an ultrasonic bath. The ultrasonics had little effect except to disperse clay and so clean up the crushed nodule. The water however was dissolving something from the crushed nodule to give a yellow solution, and XRF examination of the evaporate showed V and As, Se, Mo and Br (in order of importance). An XRF scan of a cut surface of the nodule showed V, As, Cu, Se, Co, Ni, U, Ge and Ti to be present (no Ag). An XRD powder film of one of the silvery-white particles picked out of a cut surface showed metadomehite ( $\text{Cu}_3\text{As}$ ) (film No. Ph 7180).

The XRF results are very much approximations to the composition of the inhomogeneous nodules. Cut sections of the nodules (except two of the "whole rock" measurements, where elvacite-bound discs were used) were presented to the XRF. Since local concentrations of an element may be missing from the surface layer measured for an element it is very much a matter of chance whether or not the XRF result is representative of the nodule. Despite this caution certain conclusions can tentatively be drawn from the correlation coefficient matrix (in which the significant correlations are highlighted). Uranium is correlated with As, Cu and Co. However Cu and Co are also more highly correlated so one or other correlation with U is likely to be indirect. The Co v U correlation is higher than Cu v U, which suggests that these correlations are better explained by the possible presence of a cobalt-zippeite or meta-kircheimerite phase rather than postulating the presence of meta-torbernite, and that the Cu v U is a consequence of the high Co v Cu correlation, itself probably resulting from the presence of sulphides. The As v U correlation suggests that a phase such as zeunerite or trogarite might be present. Cu is correlated with Pb, As, Se and Co which is probably explained by the widespread occurrence of arsenides, selenides and sulphides of these elements.

The nodules as a whole are highly variable, no two being alike and the use of a mean or even the median for the batch should be treated with caution. The absence of significant correlations of V with any other element suggests that the majority of the V is present as phase/s independent of the other elements examined.

D.J. Bland  
23/4/85

Table 1 (ppm)

## Data Matrix for NODULES FORM NEAR AND AT LITTLEHAM COVE (Semiquantitative)

	Y	SR	U	RB	TH	PB	AS	SE	ZN	CU	CO	V
8000a	630	70	7100	240	10	3000	4300	1600	390	15000	1900	36000
b	340	80	1800	260	15	15	70	10	440	970	70	15000
c	350	70	4200	230	10	3300	6100	1800	340	26000	2800	38000
d	80	100	1400	290	10	370	5000	80	380	980	1800	21000
e	130	110	1200	330	10	460	2000	1200	270	2300	1100	67000
f	160	70	1300	280	10	3200	4200	1500	1300	17000	1200	48000
8009	160	80	20	240	10	290	120	nd	410	740	40	11000
8010	10	20	30	200	10	180	20	nd	580	1100	nd	6000
8014	30	50	20	200	15	40	10	nd	190	190	60	7100
8023	40	150	4	280	20	15	15	nd	110	30	60	300
8026	15	60	20	220	10	110	10	nd	230	60	40	8000
8045	30	80	30	200	15	1600	140	10	410	810	80	15000
8046	760	90	80	260	5	2800	120	30	680	2500	150	24000

nd = not detected

Table 2 (ppm)

## Other elements detected, some with semiquantitative values

	Ba	Cs	Sb	Cd	Ag	Mo	Ti	Ge	Ni
HBR 8000a	+			200	800				++
HBR 8000b	+								+
HBR 8000c	+		15	30	960		+		+
HBR 8000d	+	+	50			170			++
HBR 8000e	+	+						?	+
HBR 8000f	+	?		240	600				+
HBR 8009	+	+							?
HBR 8010	+							+	
HBR 8014	+	+							?
HBR 8023	+	?							
HBR 8026	+	+							?
HBR 8045	+	?							
HBR 8046	+	?							

+ indicates detected ++ indicates much detected ? perhaps

Table 3 Semiquantitative "whole rock" data

Sample No.	ppmNi	%Fe <sub>2</sub> O <sub>3</sub>	%MnO	%CR <sub>2</sub> O <sub>3</sub>	%TiO <sub>2</sub>	ppmBa	%CaO	%K <sub>2</sub> O
HBR 8023	50	7.21	0.107	0.012	0.892	417	3.48	4.82
HBR 8000A	81	1.31	0.080	0.235	0.537	243	6.79	4.41
HBR 8000B	169	1.51	0.070	0.298	0.550	283	6.50	5.11

Table 3 continued

Sample No.	ppmCl	ppmS	%P <sub>2</sub> O <sub>5</sub>	%SiO <sub>2</sub>	%Al <sub>2</sub> O <sub>3</sub>	%MgO	%Na <sub>2</sub> O	Total
HBR 8023	72	221	0.141	50.9	16.2	2.61	0.4	86.8
HBR 8000A	706	433	0.099	54.6	9.63	1.66	0.5	80.0
HBR 8000B	548	884	0.099	57.3	9.79	1.68	0.5	83.5

Table 4a Correlation Coefficient Matrix for NODULES FROM NEAR AND AT LITTLEHAM COVE.

	Y	SR	U	RB	TH	PB	AS	SE	ZN	CU	CO
SR	0.05										
U	0.56	-0.06									
RB	0.14	0.71	0.08								
TH	-0.51	0.37	-0.18	-0.09							
PB	0.65	-0.09	0.58	0.01	-0.47						
AS	0.24	0.04	<u>0.71</u>	0.31	-0.32	-0.62					
SE	0.09	-0.40	0.67	0.10	-0.21	0.59	0.71				
ZN	0.22	-0.28	0.01	0.13	-0.44	0.56	0.26	0.15			
CU	0.40	-0.15	<u>0.72</u>	0.02	0.28	<u>0.83</u>	<u>0.81</u>	<u>0.87</u>	0.38		
CO	0.27	-0.09	<u>0.76</u>	0.23	-0.35	0.59	<u>0.97</u>	0.75	0.18	<u>0.81</u>	
V	0.31	0.13	0.46	0.61	-0.44	0.53	0.61	0.73	0.36	0.55	0.61

Significant Values in C.C. Matrix

..... = Probability at 99% Confidence Level

\_\_\_\_\_ = Probability at 99.9% Confidence Level.

Table 4b (ppm)

NODULES FROM NEAR AND AT LITTLEHAM COVE

	Number of Values	Average of Input Values	Standard Deviation	Median of Input Values
Y	13	210	244	130
SR	13	79	31	80
U	13	1323	2114	80
RB	13	248	40	240
TH	13	12	4	10
PB	13	1183	1379	370
AS	13	1700	2324	120
SE	8	779	815	10
ZN	13	441	300	390
CU	13	5206	8434	980
CO	12	775	962	80
V	13	22877	19363	16000



3

SCU

2

1

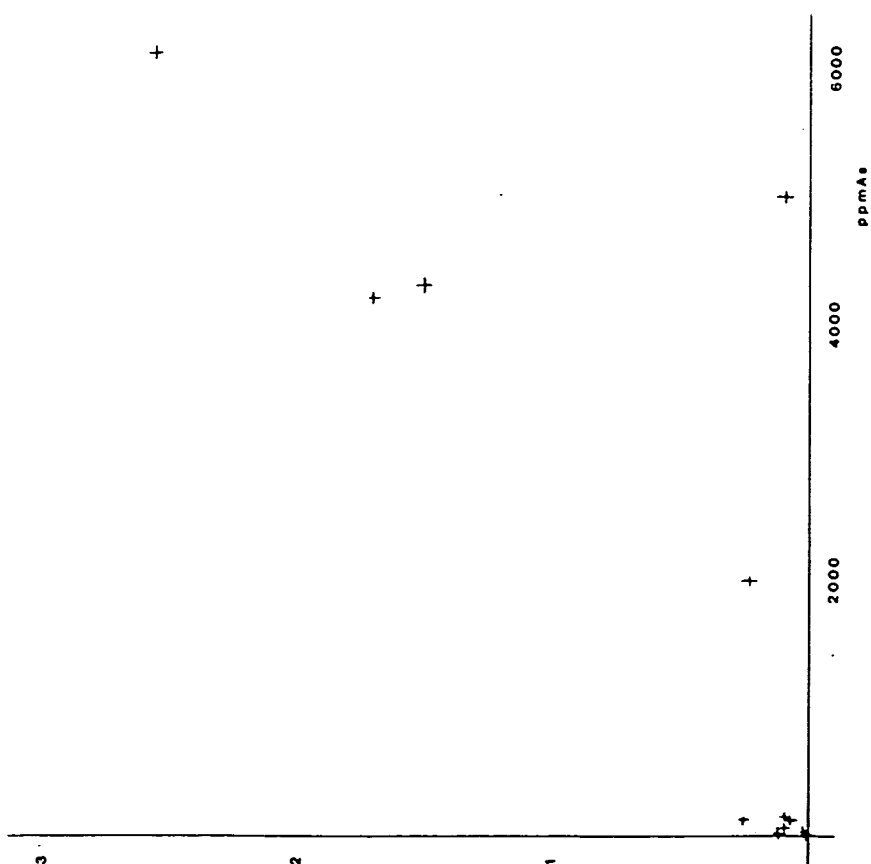


Figure 3



Figure 4